UDK 669.1:621.791.763:52-334.2
Original scientific article/Izvirni znanstveni članek

ISSN 1580-2949
MTAEC9, 58(2)121(2024)

STUDYING THE STRENGTH OF DISSIMILAR JOINTS OF AISI 430 AND 301 STAINLESS STEEL WELDED AT DIFFERENT WELDING PARAMETERS

TRDNOST ZVARNIH SPOJEV MED NERJAVNIMA JEKLOMA VRSTE AISI 430 IN 301 V ODVISNOSTI OD RAZLIČNIH PARAMETROV VARJENJA

Sedat Aras*, Rukiye Ertan

Bursa Uludag University, Automotive Engineering Department, Bursa 16059, Turkey

Prejem rokopisa – received: 2023-12-03; sprejem za objavo – accepted for publication: 2024-01-16

doi:10.17222/mit.2023.1054

Investigating the best welding parameters for resistance spot welding joints between AISI 430 and AISI 301 stainless steels was the primary focus of this study. This research involved welding samples of these stainless steel types using various welding parameters. Ferritic stainless steel (AISI 430) and austenitic stainless steel (AISI 301) were subjected to resistance spot welding, and different welding conditions were applied to produce a range of samples. The study specifically analyzed the influence of the welding current (2.5, 3.1 and 3.7) kA and welding time (40, 70 and 100) ms on the joining capability of these stainless steels. To determine the best welding parameters, microhardness measurements and tensile-shear tests were performed on the welded materials. The results indicated that increasing the welding current and welding time led to an increase in the tensile load. The maximum tensile-shear load 2036 N was observed at 3.7 kA and 100 ms. However, after a salt spray test (48 and 96) h, a serious decrease in the tensile load from 2036 N to 750 was observed at the high current 3.7 kA and time (70 and 100) ms. At 3.1 kA and 70 ms before and after the salt test, its value remained relatively constant, and the corrosion resistance of the weld joint was at the best level. The microhardness of the heat-affected zone increased, reaching its maximum point (for 3.1 kA and 70 ms: 347.3 HV and for 3.1 kA 100 ms: 369 HV) in the fusion zone. Moreover, the increase in the welding time and current was associated with an increase in the nugget size. The maximum nugget size was 3.61 mm at 3.7 kA and 100 ms.

Keywords: stainless steel, resistance spot welding, corrosion resistance, mechanical properties, welding parameter

V članku avtorja opisujeta vpliv parametrov uporovnega točkovnega varjenja na lastnosti zvarnih spojev med feritnim nerjavnim jeklom vrste AISI 430 in austenitnim nerjavnim jeklom vrste AISI 301. Za raziskavo sta izdelala ustrezne preizkušance iz obeh vrst jekla in jih medsebojno zvarila pri različnih parametrih uporovnega točkovnega varjenja. V študiji sta avtorja analizirala vpliv jakosti električnega toka varjenja (2,5 kA, 3,1 kA in 3,7 kA) ter časa varjenja (40 ms, 70 ms in 100 ms) na sposobnost spajanja dveh medsebojno mikrostrukturno različnih vrst nerjavnih jekel. Zato, da bi določila najboljše parametre varjenja sta avtorja na zvarjenih preizkušancih določila njihovo mikrotrdoto in natezno-strižno trdnost. Rezultati meritev so pokazali, da z naraščajočo jakostjo električnega toka in časa varjenja narašča tudi natezna trdnost oz. obremenitev potrebna za porušitev zvarnih spojev. Maksimalna natezno-strižna obremenitev (2036 N) je bila dosežana pri 3,7 kA in 100 ms. Vendar pa so nadaljni korozijski preizkusi naprševanja zvarov s slanico (48 in 96ur) pokazali močno zmanjšanje trdnosti teh spojev. Tako je natezna obremenitev pri porušitvi preizkušancev padla z 2036 N na 750 N pri parametrih varjenja 3,7 kA in 100 ms. Pri parametrih 3,1 kA in 70 ms pa je obremenitev pri porušitvi preizkušancev pred in po testu naprševanja s slanico ostala relativno nespremenjena. Mikrotrdota v toplotno vplivani coni je naraščala in dosegla svoj maksimum v coni taljenja; to je pri parametrih varjenja 3,1 kA in 70 ms: 347,3 HV ter pri 3,1 kA in 100 ms: 369 HV. Nadalje je bilo povečanje jakosti toka in časa varjenja povezano tudi s povečanjem velikosti zvarnih točk (angl.: nugget size) . Maksimalna izmerjena velikost zvarnih točk je bila 3,61 mm pri 3,7 kA in 100 ms.

Ključne besede: nerjavno jeklo, uporovno točkovno varjenje, odpornost proti koroziji, mehanske lastnosti, parametri varjenja.

1 INTRODUCTION

In recent years, there has been a consistent rise in the use of stainless steel across various industrial sectors, including automotive sector, white goods, and medicine. Stainless steels are particularly favored for their outstanding corrosion resistance, appealing esthetics, commendable toughness, satisfactory weldability and formability. They exhibit superior corrosion resistance and greater energy absorption than carbon steels. It is noteworthy that the strength of stainless steels is relatively modest in the annealed state, which poses a limitation for certain applications.[1–3]

Austenitic stainless steel is the most widely used type, but its prevalence is hindered by the high cost of Ni. In contrast, ferritic stainless steels, which are devoid of Ni, present a cost-effective alternative with high thermal conductivity and superior resistance to stress corrosion cracking. The integration of hybrid austenitic and ferritic stainless steels provides a potential solution for reducing the Ni usage. Achieving this hybrid structure involves employing various joining processes for austenitic and ferritic stainless steels. The intricate metallurgical reactions, stemming from the high proportion of alloying elements in stainless steel, make the welding

*Corresponding author's e-mail:
arassdt@gmail.com (Sedat Aras),
ORCID number: 0000-0002-5651-3484

Table 1: Chemical compositions of AISI 430 ferritic stainless steel and AISI 301 austenitic stainless steel (*w*/%)

	Fe	Cr	Ni	Mn	Si	C	P	S
AISI 430	Bal.	17.5	0.141	0.769	0.471	0.12	–	0.01
AISI 301	Bal.	16.71	6.89	1.16	0.54	0.08	0.02	0.003

process more complex than that of carbon structural steel counterparts. Forecasting the phase transformation of stainless steel welds can be facilitated by examining constitution diagrams, such as the Schaeffler diagram,[4,5] the WRC-1992 diagram[6] and the Balmforth diagram.[7] Welded joints of ferritic and austenitic stainless steels are widely used in industrial applications, including power plants, energy conversion systems and nuclear domains. The AISI 301 austenitic stainless steel, renowned for its superior corrosion resistance, strength and ductility serves as a structural material in diverse sectors such as the chemical and aviation industries.[8,9] On the other hand, among ferritic stainless steels, the AISI 430 type with a 17 % chromium content is the most extensively employed variant in various fields. Given these considerations, delving into the welding of both austenitic and ferritic stainless steel becomes paramount.[10,11]

Resistance spot welding has emerged as the predominant method for joining sheet materials, and has found extensive use in the welding of low-carbon steel, stainless steel and aluminum. Being particularly advantageous in situations where disassembly is not required, resistance spot welding is often the preferred choice over mechanical fasteners. Its versatile application spans industrial sectors, maintenance fields, automobile manufacturing and the nuclear industry.[12–14] Distinguished by its simplicity and suitability for automation, resistance spot welding relies on relatively straightforward equipment. Once best welding parameters are established, this method becomes highly suitable for mass production purposes.[15–17]

The most important feature of stainless steels is their resistance to corrosion. The corrosion resistance of combinations of stainless steels with different properties varies. Dissimilar joints were also found to exhibit high corrosion current density because of the effect of galvanic corrosion. Because of the mixing of dissimilar metals, a dissimilar joint with a chemical composition and microstructure that are significantly different from the base metal was produced. The differences in the chemical composition and microstructure may induce severe galvanic corrosion, leading to accelerate corrosion damage. It is also known that small weld defects, pores, cracks and inclusions are easily attacked by an aggressive solution, causing an increasing corrosion susceptibility of a joint.[5] Therefore, it is necessary to investigate the corrosion mechanism of dissimilar joints. Corrosion resistance of stainless steels is evaluated with different corrosion tests.

M. H. Bina et al.[15] investigated the effect of the welding time on resistance spot welded dissimilar stainless steels and concluded that the tensile shear load of the welded samples increased with the welding time. In addition, as the welding time was increased the nugget diameter increased on both sides. C. Wang et al.[8] explored the corrosion behavior of dissimilar 304 and 430 stainless steel welded joints. They concluded that the corrosion resistance of the welded joints first decreased with an increasing fusion ratio of AISI 304, and later increased with further increase in AISI 304. During the former stage, the reduced anti-corrosive property of the weld is due to the formation of larger portions of martensite and phase boundaries; during the latter stage, an increased Cr content and decreased fraction of the phase boundary are responsible for the improvement in the anti-corrosive property of the welded joint. Y. Zanga et al.[4] investigated the mechanical and microstructural properties of resistance spot welding joints between ferritic AISI 430 and austenitic AISI 304 stainless steel. They reported that the microhardness of the nugget of 304 and 430 is higher than that of the base metals. This is due to the generation of martensite in the nugget.

With the research, we determined the best welding time and welding current for resistance spot welding joints between AISI 430 and AISI 301 stainless steel. In this scope, the mechanical properties of the weld joint were evaluated with a tensile-shear test, microstructure analysis and salt spray test. The salt spray test was applied to evaluate the corrosion resistance of the joint after welding, which was also evaluated with the tensile-shear test after the salt spray test.

2 EXPERIMENTAL PART

2.1 Materials and methods

In this investigation, AISI 430 ferritic stainless steel and AISI 301 austenitic stainless steel were selected as the base metals, each with a thickness of 0.4 mm. Detailed information regarding the chemical compositions of these steels is provided in **Table 1**.

Table 2: Constant welding parameters

Electrode type	Wirbalit B CuCoBe (D16×20)
Electrode pressure	3 bar
Current tolerance	± 2.5
Pressure tolerance	± 5
Diode temperature	34 °C
Switch-of temperature	150 °C

Resistance spot welds were created using various welding parameters, including welding currents of (2.5,

3.1 and 3.7) kA, and welding times of (40, 70 and 100) ms. Throughout the welding process, the electrode pressure was maintained at 3 bar while other parameters were kept constant. They are shown in **Table 2**. The welding operations were performed using Bosch Rexroth PRC7300 equipment with Wirbalit B CuCoBe (D16×20) electrodes.

2.2 Test procedure

Tensile-shear tests were performed using a Zwick Roell Z020 machine in accordance with EN ISO 6892, with a test speed of 0.0067 1/s. Welded parts, prepared based on the guidelines of DIN EN ISO 14273, had standard dimensions of 105 mm in length and 45 mm in width, with a joint overlap of 35 mm.

Tensile-shear tests were performed before and after the salt spray corrosion test of the weld joints. Salt spray tests, performed in accordance with ISO 9227, involved exposure for 48 h and 96 h.

The weld-nugget size of the weld joints was measured using a caliper before the tensile-shear test. Vickers microhardness tests were carried out on the welded samples using a Struers Duramin hardness tester. The loading applied during the measurements was set at 200 g for a duration of 5 s. The schematic representation in **Figure 1** shows the hardness measurement points and the direction of the weld joint.

3 RESULTS AND DISCUSSION

3.1 Nugget-diameter changes

Resistance spot welding is influenced by various crucial factors that impact the weld quality, including the surface view of the nugget, its strength, ductility, size, penetration, sheet separation and internal discontinuities.[8–12] Ideally, a spot weld should exhibit a relatively smooth, round, or oval surface, especially in contoured work, and should be free from surface fusion, electrode deposit pits, cracks and deep electrode indentation. **Figure 2** shows the nugget surface appearance for different welding currents (2.5, 3.1, 3.7) kA and times (40, 70, 100) ms, along with the corresponding diameter of each nugget for welded dissimilar materials. These findings indicate that the weld-nugget size increases with a higher welding current and longer welding time. Specifically, the samples produced at 3.7 kA and 100 ms show the largest nugget diameter. However, there is a limit to the increase in the nugget diameter. Further increments in the welding current beyond this limit reduces the nugget diameter due to excessive metal melting and splashing in the interlayer.

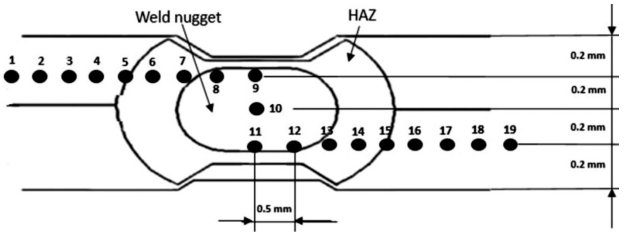

Figure 1: Hardness points and measurement direction of the welded joint

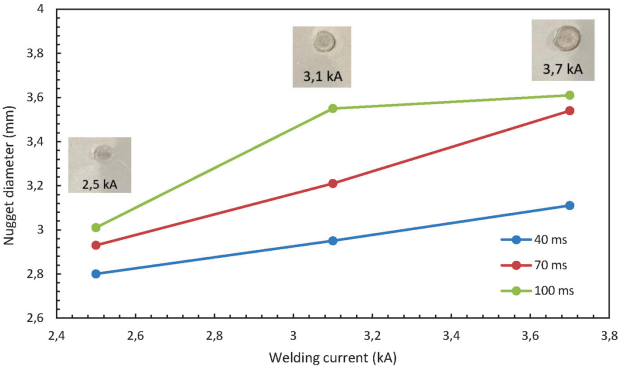

Figure 2: Nugget surface appearance for 2.5, 3.1 and 3.7 kA and the diameters of the nuggets of the welded dissimilar materials related to the welding current and time

3.2. Tensile-shear test results

Before the salt-spray test, the outcomes of the welded joints indicated that the tensile-shear peak loads of the welded samples increased with the welding current and time. The maximum peak load for the joints was observed at the welding current of 3.7 kA and welding time of 100 ms, reaching a value of 2036 N.

The most important feature of stainless steel is its superior corrosion resistance. Therefore, this study investigated the corrosion resistance of dissimilar stainless-steel welds, specifically a combination of austenitic and ferritic steels. Tensile-shear tests were performed after 48 h and 96 h of the salt-spray tests, and the results are shown in **Figures 3** and **4**.

In this research, all the welded samples were tensile-shear tested in order to evaluate the weld quality. Based on the results of the tensile-shear tests, the salt-spray test was applied to the joints welded at the welding currents, resulting in high tensile-shear peak-load values. The focus was on the best results obtained under the welding tensile load at the welding cur-

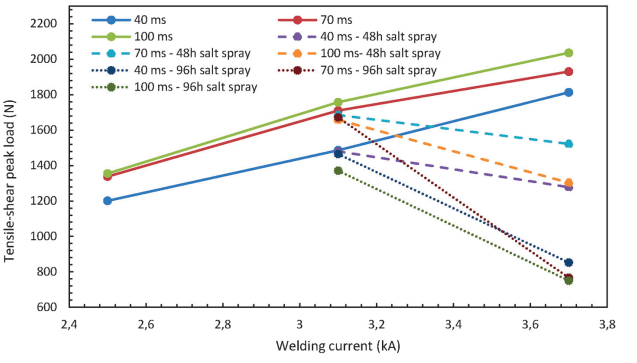

Figure 3: Tensile-shear test results before and after the salt spray test for 48 h and 96 h of the joints related to the welding current and time

Table 3: Tensile-shear test results

Welding current (kA)	40 ms	70 ms	100 ms	40 ms – 48 h salt spray	70 ms – 48 h salt spray	100 ms – 48 h salt spray	40 ms – 96 h salt spray	70 ms – 96 h salt spray	100 ms – 96 h salt spray
2,5	1201 N	1338 N	1355 N	–	–	–	–	–	–
3,1	1486 N	1710 N	1757 N	1480 N	1685 N	1658 N	1465 N	1672 N	1371 N
3,7	1813 N	1930 N	2036 N	1278 N	1522 N	1303 N	852 N	766 N	750 N

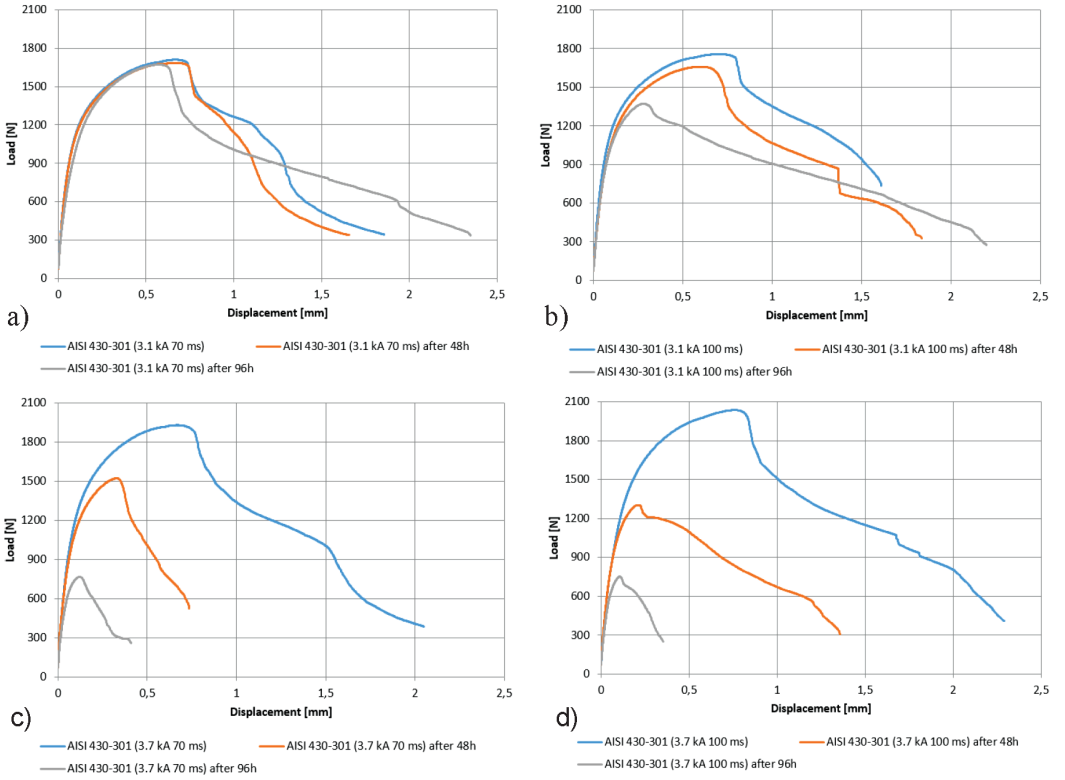

Figure 4: Tensile-shear load-displacement results for the AISI 430-AISI 301 welded samples before and after the salt spray test: a) 3.1 kA and 70 ms, b) 3.1 kA and 100 ms, c) 3.7 kA and 70 ms, d) 3.7 kA and 100 ms

rents of (3.1 and 3.7) kA and welding times of (40, 70 and 100) ms.

At 2.5 kA and 40 ms, 70 ms and 100 ms, the results were lower than at other parameter values, as shown in **Table 3** and highlighted in purple. Separation-type breaking was seen, as shown in **Figures 5** and **6**. A fragile interfacial failure occurred and the breaking force was very low. The joint was not fully formed and the welding time and current were insufficient, so due to the low welding current and time, there was a low heat input. For this reason, these values were not used in further tests, including salt spray tests. The values of 3.1 kA and 70 ms and 3.1 kA ms and 100 ms were selected for the microhardness analyses as the resulting peak-load reductions were lower than in other cases.

The spot-welded sheets were exposed to a salt spray for 48 h and 96 h, followed by tensile-shear tests. The results indicated significant decreases in the peak load after the salt-spray test, which were especially high at the welding current of 3.7 kA.

A high welding current and welding time may cause defects in a weld nugget; internal discontinuities include cracks, porosity, big cavities and metallic inclusions. These internal defects in a spot weld may also be caused by any other conditions that produce excessive weld heat.[15–18] Due to high thermal expansion, high welding shrinkage strains can be responsible for these internal defects. In this research, the salt-spray test may have caused the tensile-shear load to decrease significantly at the high current and high time values due to these internal defects.

If the welding current was high and consequently the thermal stresses were high, the pitting that appeared on the surface was more intense and so was the corrosion rate. So, an increased welding current of resistance spot welding leads to increased pitting and corrosion rate.[19] The microstructure of the HAZ and fusion zone becomes coarser and dendritic with an increasing welding-heat input. The corrosion rate of welded joints increases with an increasing heat input.[20]

For these reasons, it is believed that there is a decrease in the tensile-shear load after the salt test at high current and time values: 3.7 kA and (40, 70 and 100) ms and also 3.1 kA and 100 ms.

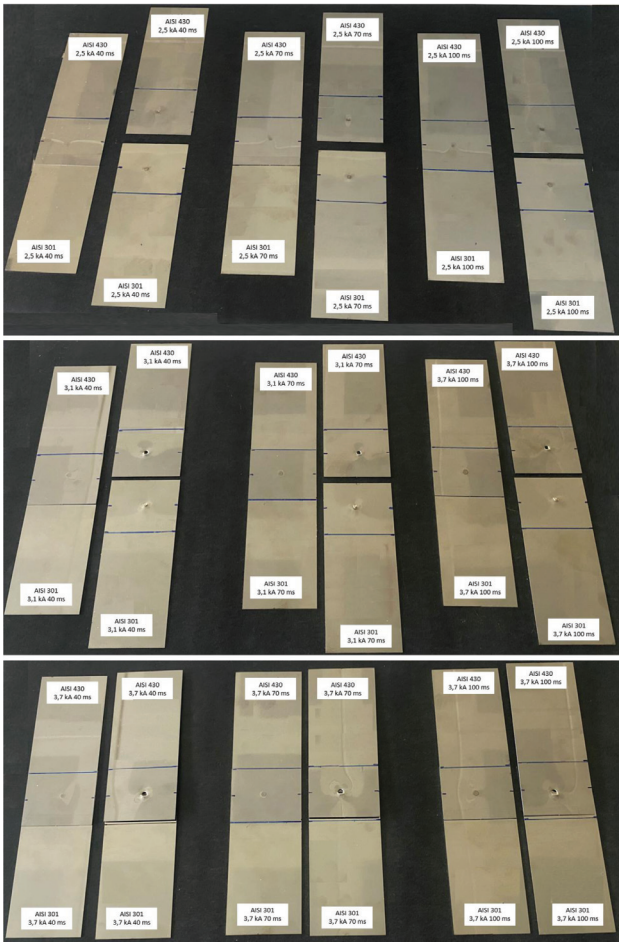

Figure 5: Views of samples AISI 430-AISI 301 before and after the tensile-shear test: a) 2.5 kA, 40 ms, 70 ms, 100 ms, b) 3.1 kA, 40 ms, 70 ms, 100 ms, c) 3.7 kA, 40 ms, 70 ms, 100 ms

From **Figures 3** and **4**, it is evident that the welding current of 3.7 kA is sufficiently high to substantially diminish the corrosion resistance and load-carrying capacity of the welded stainless steel joints. A decrease was also observed at the welding current of 3.1 kA and welding time of 100 ms.

As explained above, there was a decrease in the tensile-shear load after the salt test at high current and time values. But the tensile-shear load remained relatively constant after the salt spray test at the current of 3.1 kA and welding time of 70 ms. These results are shown in **Table 3** where the results for 3.1 kA and 70 ms are highlighted in blue as the best parameter values.

Figure 5 shows that the failure is initiated on the ferritic stainless-steel side of each joint, and it is generally expected that failure occurs in the softer region of a spot weld during the tensile-shear test.

Three types of fractures were observed after the tensile-shear test: separation, knotting and tearing. **Figures 5** and **6** show photos of examples with different fractures.

In the case of the separation-type fracture, a fragile interfacial failure occurred and the breaking force was very low. The joint between AISI 430 and AISI 301 was not fully formed as the welding time and current were insufficient. Due to the low welding current and time, a low heat input was created. In the case of separation, an insufficient weld core diameter and insufficient weld zone occurred.

In the case of the knotting-type fracture, a sudden break due to a button pullout was observed, showing that the welding parameters were not suitable. The heat input increased with the welding time and welding current, the weld-core diameter and weld zone increased, and the tensile shear load also increased.

In the case of the tearing-type fracture, a tear in the material propagated until it became a sharp fracture in the welded area. It is observed at the circumference of the molten zone.

3.3 Microhardness measurements

The tensile-test results of the welded samples subjected to salt spray were evaluated, and it was determined that, considering the tensile forces before and after the salt test, the best results were seen at 3.1 kA. That is why we focused on this value for microhardness. Therefore, microhardness measurements were taken on the samples welded at the 3.1 kA welding current and 70 ms and 100 ms welding times. On **Figure 7**, it can be seen that the hardness of the nuggets of all the samples is higher than that of the base metals. The increase in the welding time and current resulted in the coarsening of the microstructure of the weld nugget and also of the HAZ. This shows that martensite may have formed in the weld nugget.[4,15,21] For the joints of austenitic and ferritic stainless steel, the microhardness distribution was almost the same at different welding times (70 ms and 100 ms).

The microhardness measurement was carried out on the weld nugget – the fusion zone (FZ), heat affected zone (HAZ) and base material (BM), as shown in **Figure**

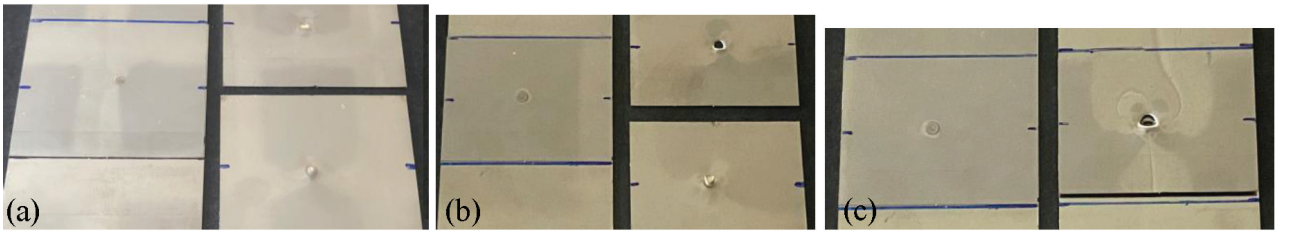

Figure 6: Examples of tensile-shear test samples with fractures: a) 2.5 kA and 70 ms, b) 3.1 kA and 70 ms, c) 3.7 kA and 70 ms

Figure 7: Microhardness change with 70 ms and 100 ms welding times and 3.1 kA welding current for AISI 430-AISI 301 welded joints

7. This shows that the microhardness of the nuggets of all the samples is higher than that of the base metals, which may be due to the formation of martensite in the weld nugget.[4–15]

4 CONCLUSION

The purpose of this study was to determine the best resistance spot welding parameters, focusing specifically on variable parameters such as the welding current and welding time, for dissimilar steels, AISI 301 and AISI 430.

Various properties of resistance spot welds of dissimilar steels obtained at different welding parameters were systematically investigated. The principal conclusions derived from this study are summarized as follows:

The findings indicated that at values of 2.5 kA and (40, 70 and 100) ms the results were lower than at other parameter values. So, the focus was on the values, at which the welding tensile load gave the best results, i.e., the welding currents of (3.1 and 3.7) kA and welding times of (40, 70 and 100) ms. The tensile-shear load of the welded samples increased with the welding current, but significant drops in the tensile strength were observed at the current value of 3.7 kA and welding-time values of (40, 70 and 100) ms after the salt-spray test. A decrease was also observed at the current of 3.1 kA and welding time of 100 ms, especially after 96 h. At the current of 3.1 kA and welding time of 70 ms, the tensile-shear load remained constant after the salt-spray test.

In accordance with the tensile-shear test results before and after (96 h) the salt-spray test, the following data can be recorded:

3.1 kA, 40 ms → Before: 1486 N – After: 1465 N
3.1 kA, 70 ms → Before: 1710 N – After: 1672 N
3.1 kA, 100 ms → Before: 1757 N – After: 1371 N
3.7 kA, 40 ms → Before: 1813 N – After: 852 N
3.7 kA, 70 ms → Before: 1930 N – After: 766 N
3.7 kA, 100 ms → Before: 2036 N – After: 750 N

The microhardness of the sample nuggets is higher than that of the base metals. According to the tensile-shear test results (before and after the salt-spray test) the parameter values of 3.1 kA and 70 ms and 3.1 kA and 100 ms were selected for the microhardness analyses.

The microhardness of the heat-affected zone increased, reaching its maximum values in the fusion zone, at 3.1 kA and 70 ms: 347.3 HV and at 3.1 kA and 100 ms: 369 HV.

The results indicated a positive correlation between the increasing welding current and time and an increase in the nugget size, attributed to the heightened heat input. The observed types of fracture of the welded samples included separation, knotting and tearing. With the low welding current 2.5 kA and (40, 70 and 100) ms, separation was observed; with the higher welding currents and welding times, tearing (3.7 kA and 40, 70, 100) ms and knotting 3.1 kA and (40, 70, 100) ms were observed.

Based on the test results, the optimum welding current and time in resistance spot welding of AISI 430 and AISI 301 stainless steel, in terms of mechanical properties, were 3.1 kA and 70 ms.

5 REFERENCES

[1] D. Ozyurek, An effect of weld current and weld atmosphere on the resistance spot weldability of 304L austenitic stainless steel, Mater. Design, 29 (**2008**) 3, 597–603, doi:10.1016/j.matdes.2007.03.008

[2] A. E. Reiter, B. Brunner, M. Ante, J. Rechberger, Investigation of several PVD coatings for blind hole tapping in austenitic stainless steel, Surf. Coat. Tech., 200 (**2006**) 18–19, 5532–5541, doi:10.1016/j.surfcoat.2005.07.100

[3] H. B Carry, Modern Welding Technology, 2nd Edition, American Welding Society, Prentice Hall 1981

[4] Y. Zhanga, J. Guob, Y. Li, Z. Luo, X. Zhang, A comparative study between the mechanical and microstructural properties of resistance spot welding joints among ferritic AISI 430 and austenitic AISI 304 stainless steel, J. Mater. Res. Tech., 9 (**2020**) 1, 574–583, doi:10.1016/j.jmrt.2019.10.086

[5] J. Verma, R. V. Taiwade, Effect of welding processes and conditions on the microstructure, mechanical properties and corrosion resistance of duplex stainless steel weldments—A review, J. Manuf. Process., 25 (**2017**), 134–152, doi:10.1016/j.jmapro.2016.11.003

[6] D. J. Kotecki, T. A. Siewert, WRC-1992 Constitution Diagram for Stainless Steel Weld Metals: A modification of the WRC-1988 Diagram, Welding Research Supplement, 71 (**1992**) 5, 171–178

[7] M. C. Balmforth, J. C. Lippold, A New Ferritic-Martensitic Stainless Steel Constitution Diagram, Supplement to The Welding Journal, 79 (**2000**) 12, 339–345

[8] C. Wang, Y. Yu, J. Yu, Y. Zhang, Y. Zhao, Q. Yuan, Microstructure evolution and corrosion behavior of dissimilar 304/430 stainless steel welded joints, J. Manuf. Process., 50 (**2020**), 183–191, doi:10.1016/j.jmapro.2019.12.015

[9] M. Sireesha, V. Shankar, Microstructural Features of Dissimilar Welds between 316LN Austenitic Stainless Steel and Alloy 800, Mater. Sci. Eng., 292 (**2000**) 1, 74–82, doi:10.1016/S0921-5093(00)00969-2

[10] M. S. Khorrami, M. A. Mostafaei, H. Pouraliakbar, A. H. Kokabi, Study on Microstructure and Mechanical Characteristics of Low Car-

bon Steel and Ferritic Stainless Steel Joints, Mater. Sci. Eng., 608 (**2014**), 35–45, doi:10.1016/j.msea.2014.04.065

[11] G. Senthilkumar, V. Vinodkumar, T. Mayavan, G. Rathinasabapathi, A. G. David, Optimization of process parameters for a solid-state-welded AISI 430 steel joint with the GRG reinforced response surface methodology, Mater. Tech., 57 (**2023**) 5, 485–494, doi:10.17222/mit.2023.873

[12] S. B. Jamaludin, M. Hisyam, Study of spot welding of austenitic stainless steel type 304, J. Appl. Sci. Res., 3 (**2007**) 11, 1494–1499, doi:10.13140/2.1.4207.0400

[13] M. Vural, A. Akkus, On the Resistance Spot Weldability of Galvanized Interstitial Free Steel Sheets with Austenitic Stainless Steel Sheets, J. Mat. Process. Tech., 153–154 (**2004**), 1-6, doi:10.1016/j.jmatprotec.2004.04.063

[14] E. Bayraktar, D. Kaplan, M. Grumbach, Application of impact tensile testing to spot welded sheets, J. Mat. Process. Tech., 153–154 (**2004**), 80–86, doi:10.1016/j.jmatprotec.2004.04.020

[15] M. H. Bina, M. Jamali, M. Shamanian, H. Sabet, Effect of Welding Time in the Resistance Spot Welded Dissimilar Stainless Steels, Trans. Indian. Inst. Met., 68 (**2015**) 2, 247–255, doi:10.1007/s12666-014-0452-1

[16] M. Alizadeh-Sh, S. P. H. Marashi, M. Pouranvari, Resistance spot welding of AISI 430 ferritic stainless steel: Phase transformations and mechanical properties, Mater. Design, 56 (**2014**), 258–263, doi:10.1016/j.matdes.2013.11.022

[17] S. Aslanlar, A. Ogur, U. Ozsarac, E. Ilhan, Welding time effect on mechanical properties of automotive sheets in electrical resistance spot welding, Mater. Design, 29 (**2008**) 7, 1427–1431, doi:10.1016/j.matdes.2007.09.004

[18] B. Kocabekir, R. Kacar, S. Gunduz, F. Hayat, An effect of heat input, weld atmosphere and weld cooling conditions on the resistance spot weldability of 316L austenitic stainless steel, J. Mater. Proc. Tech., 195 (**2008**) 1, 327–335, doi:10.1016/j.jmatprotec.2007.05.026

[19] S. M. Hassoni, O. S. Barrak, M. I. Ismail, S. K. Hussein, Effect of Welding Parameters of Resistance Spot Welding on Mechanical Properties and Corrosion Resistance of 316L, Mat. Res., 25 (**2022**) 2, doi:10.1590/1980-5373-mr-2021-0117

[20] S. P. Ambade, A. Sharma, A. P. Patil, Y. M. Puri, Effect of welding processes and heat input on corrosion behaviour of Ferritic stainless steel 409M, Mat. Proc., 41 (**2021**) 5, 1018–1023, doi:10.1016/j.matpr.2020.06.251

[21] H. G. Mohammed, T. L. Ginta, M. Mustapha, The investigation of microstructure and mechanical properties of resistance spot welded AISI 316L austenitic stainless steel, Mat. Proc., 46 (**2021**) 4, 1640–1644, doi:10.1016/j.matpr.2020.07.258